Chemical Physics 128 (1988) 135–155
North-Holland, Amsterdam

OPTICAL DEPHASING IN GLASSES: THEORETICAL COMPARISON OF THE INCOHERENT PHOTON ECHO, ACCUMULATED GRATING ECHO, AND TWO-PULSE PHOTON ECHO EXPERIMENTS

Y.S. BAI
Department of Physics and Department of Chemistry, Stanford University, Stanford, CA 94305, USA

and

M.D. FAYER
Department of Chemistry, Stanford University, Stanford, CA 94305, USA

Received 1 January 1988

We present a detailed theoretical analysis of three nonlinear optical dephasing experiments, the incoherent photon echo, the accumulated grating echo, and the two-pulse photon echo. It has been believed previously that these three experiments provide the same information about optical dephasing, and therefore about a system's dynamics. In systems such as chromophores in glasses, proteins, liquids, or complex crystals, in which spectral diffusion (slow time scale energy fluctuations) as well as homogeneous dephasing (fast time scale energy fluctuations) occur, it is proven that these techniques are not equivalent. While the two-pulse photon echo measures the homogeneous dephasing, the other two techniques are influenced by spectral diffusion. In general, the incoherent echo and the accumulated grating echo will measure dephasing rates which are faster than the two-pulse photon echo. The differences among the methods are calculated using a standard two-level system model of glasses. It is found that the differences depend on factors such as the pulse duration in the incoherent echo and the triplet life time in the accumulated grating echo. We also demonstrate that a combination of techiques can be used to map out the broad distribution of relaxation rates which occur in glasses and many other complex systems.

1. Introduction

In recent years, a variety of optical dephasing experiments have increased our knowledge of the dynamics and interactions present in both crystalline and amorphous systems [1]. An isolated molecule in a mixed crystal is surrounded by an ordered host matrix and can interact with the bulk modes of the lattice, the acoustic and optical phonons. In addition, the solute itself can undergo motions which are referred to as pseudo-local modes. In contrast, molecules in a glass experience a wide range of local environments because of the variety of structures of the solvent shells around each molecule. The local structures associated with a glassy system are not static even at very low temperatures (≈ 1 K). Small potential barriers separate different local mechanical configurations. Tunneling and thermal activation result in constantly changing solvent structures. This is in contrast to a crystal in which phonon-induced fluctuations occur about a single equilibrium lattice structure.

The constantly changing local structures in a glass cause the heat capacities of glasses to be markedly different at low temperatures than those of crystals [2]. Anderson and co-workers [3] and Phillips [4] independently proposed a model based on the two-level system (TLS) to explain these differences. TLS represent extra degrees of freedom that are characteristic of the glassy state, and they contribute a term approximately linear in temperature to the temperature dependence of the heat capacity of a glass. Briefly, a TLS is composed of two separate local potential minima separated by a barrier. Changes in local glass structure are modeled as transitions between the two potential minima. A wide distribution of energy differences of the TLS potential minima and a

0301-0104/88/$ 03.50

wide distribution of tunneling parameters are responsible for these transitions. As a result, there is a very wide range of time scales associated with the dynamics of the TLS. For example, this is manifested in the time dependence of the heat capacities of glasses [5].

The transition energies of a solute chromophore in a glass can be shifted by the variations in the local configuration. The static distribution of solvent configurations results in a very broad inhomogeneous absorption spectrum. Various nonlinear spectroscopic techniques can be used to remove inhomogeneous broadening, permitting the extraction of information on dynamics and intermolecular interactions from the dephasing of electronically excited chromophores.

Besides the static energy shift, the transition energies of the chromophores are also modulated by the tunneling TLS. The dephasing of the chromophores can be affected by processes in the medium which occur over a wide variety of time scales. The time scales can range from extremely fast phonon-induced fluctuations to much slower configurational changes, and finally to totally static inhomogeneities. Depending on the relative time scale of the experiment, the transition frequency modulations can contribute to either the inhomogeneous broadening or the dephasing of the chromophores. This is because the dephasing measured in an experiment with a relatively long time scale is affected by slow frequency modulations that appear static to and are rephased in a faster experiment. It is therefore necessary to carefully consider the sensitivity of various spectroscopic techniques to the distribution of time scales.

The most common spectroscopic techniques used to measure optical dephasing in glasses are fluorescence line narrowing [1], hole burning [1], two-pulse photon echoes [6], and accumulated grating echoes [7]. It is now clear [8] that the first two techniques are associated with much longer time scales than the time domain echo techniques. Berg et al. presented a detailed theoretical and experimental study of optical dephasing of chromophores in glasses [8]. A significant difference between the dephasing rates measured with photon echo and hole burning experiments was observed [8]. Previously, hole burning experiments had been interpreted in terms of a two-time transition dipole correlation function. Berg et al. developed the appropriate four time correlation function description for hole burning as well as other optical line narrowing experiments. It was proven that the correlation function which describes the optical line narrowing experiments applied to glassy systems is the same as correlation function that describes the stimulated echo. The stimulated echo is a well-known magnetic resonance experiment used to measure spectral diffusion. The analysis showed that different optical line narrowing experiments are sensitive to dynamics on different time scales, and therefore the results from different experimental methods will, in general, not be the same. Berg et al. presented a comprehensive evaluation of the correlation functions for hole burning and two-pulse photon echo experiments using a detailed model of glasses and compared the results to experiments [8]. This work provided an in depth understanding of the relationship between photon echo and hole burning dephasing measurements and yielded the first measurements of the temperature dependence of optical spectral diffusion in glasses.

The study presented by Berg et al. focused mainly on the two-pulse photon echo and on hole burning. Recently there has been considerable interest in the application of the incoherent photon echo technique to study dephasing in glasses and other complex systems. The incoherent photon echo, as will be demonstrated below, is closely related to the accumulated grating echo. Analysis is needed to establish the nature of the observables and the time scales which are associated with the various echo techniques.

A two-pulse photon echo is generated by the manipulation of the coherence between the two electronic states involved in the optical transition. In a two-pulse echo experiment, the second pulse is delayed from the first by a time τ. The echo occurs at a time 2τ. Any transition energy fluctuations occurring within this time frame contribute to the optical dephasing. The dephasing measured by a two-pulse photon echo is generally referred to as the homogeneous dephasing.

The excitation scheme in an accumulated grating echo experiment is distinct from that of the two-pulse photon echo. Like the two-pulse photon echo, pairs of pulses are applied to the sample. The difference is that the repetition rate of the pulse pairs is much faster in an accumulated grating echo experiment: many pairs of pulses are applied before the chromophores relax back to their ground states. The light source used in this kind of

experiments is usually a low power cw mode-locked laser. In addition to the very weak echo (generally undetectable) produced by the same mechanism as that of the two-pulse echo, each pulse pair in the stream of pulses generates population modulations on the inhomogeneous line [7]. The modulations produce a grating in frequency space, with the period of the grating given by $1/\tau$. The excited state frequency grating decays with the excited state lifetime. The ground state frequency grating, however, can last until all the chromophores relax to their ground states. This relaxation time is often determined by the lifetime of a "bottleneck" state, e.g., a triplet state. Since successive pulse pairs are applied before the chromophores relax to their ground states, the depth of the population modulations (frequency grating) will increase as the number of the pulse pairs increases. Stimulated echoes are generated by the later pulses via scattering from the frequency grating, which is an accumulated result of all previous pulse pairs. Because of the accumulative effect, these stimulated echoes dominate the detected echo signals. The important point is that, besides the characteristic time scale of the two-pulse echo, τ, the accumulated grating echo is associated with a much longer time scale, i.e. the lifetime of the bottleneck state or the lifetime of the excited state. Any energy fluctuations occurring during this time frame can contribute to the optical dephasing. In systems where slow environmental fluctuations exist, such as glasses, the dephasing rate measured with this technique will, in general, not be the same as that measured with a two pulse photon echo.

An interesting variation of the accumulated echo is the incoherent photon echo. Since first being observed in 1983 [9–11], it has been generating a great deal of interest as a new technique for the study of ultrafast optical dephasing phenomena [12]. In an incoherent photon echo experiment, the laser field is purposely made to be non-Fourier-transform limited. The time resolution is determined by the correlation time of the light source, τ_c, i.e. the inverse of its frequency bandwidth. Thus ultrahigh time resolution can easily be achieved by increasing the laser frequency bandwidth. It is often mentioned in the literature that as long as τ_c is much shorter than the sample's phenomenological dephasing time constant, T_2, the incoherent photon echo measurement should yield the same dephasing time as that measured by the two-pulse photon echo using ultrashort coherent laser pulses.

While a good deal of attention has been focused on the excellent time resolution of this new technique, little effort has been made to clarify what this technique actually measures when performed on complex systems. A central feature has been overlooked. As has been pointed out in discussing the amplitude of the signal [9], the incoherent echo is essentially an accumulated echo generated by an incoherent light source. Here the pulse pairs are composed of random modulations (coherent spikes) in the laser field. Because of its accumulative nature, however, the incoherent echo is inevitably associated with a long characteristic time scale. Just as the conventional accumulated grating echo, in systems where slow environmental fluctuations exist, the incoherent photon echo will not measure the same optical dephasing rate as the two-pulse photon echo.

Dephasing induced by relatively slow environmental fluctuations is usually referred to as spectral diffusion. The rates of these fluctuations are comparable to or slower than what is generally defined as the homogeneous dephasing rate, $1/T_2$ [8]. In crystals, spectral diffusion can be caused by spin flips in the host lattice [13–16]. The effects of spectral diffusion on the two pulse echo and the three pulse stimulated echo [13–18] measurements are drastically different. Since spectral diffusion can occur in any type of condensed matter system, particularly in disordered systems such as glasses, it is important to investigate the relationship between spectral diffusion and experimental observables to understand exactly what the incoherent photon echo and the accumulated grating echo measure.

In this article, we analyze the dephasing of an ensemble of chromophores embedded in a glassy system using the standard TLS model [1–4]. Previous investigations have shown that in this kind of system, spectral diffusion plays an important role in optical dephasing [8,19–22]. By considering the dynamic properties of the TLS and their interactions with the chromophores in some detail, we show that incoherent photon echo measurements and accumulated grating echo measurements, similar to hole burning experiments, generally result in an optical dephasing rate faster than that given by the two-pulse photon echo measurement. In some cases, the difference can be of major significance. It is also shown that using a carefully designed combination of these

techniques, one can experimentally reveal the distribution of the rates of fluctuations over a broad range of time scales.

2. The formulation of the general photon echo process

2.1. The macroscopic nonlinear polarization

Consider the interaction between a laser field and an ensemble of chromophores embedded in a glassy system. At very low temperatures, the dominant environmental fluctuations are attributed to the tunneling two-level systems [1–4]. The phenomenological Hamiltonian for an arbitrary chromophore can be written as

$$H = H_0 + H_{\text{int}} . \tag{2.1}$$

H_0 is the Hamiltonian of the glassy system in the absence of the laser field. It generally contains three terms. The first term describes the energy levels of the chromophore,

$$H_c = \sum_{\alpha} \epsilon_\alpha |\alpha\rangle\langle\alpha| .$$

The second describes the perturbation of the chromophore arising from interactions with the TLS, which can be expressed as

$$H_{\text{T.L.S-C}} = \sum_{\alpha} \sum_{j} \xi_\alpha(\boldsymbol{r}_{ij})\, \Delta\rho_j |\alpha\rangle\langle\alpha| . \tag{2.1'}$$

The chromophore is labeled with index i. $\xi_\alpha(\boldsymbol{r}_{ij})$ is the coupling strength between the jth TLS and the state $|\alpha\rangle$ of the chromophore. $\boldsymbol{r}_{ij} = \boldsymbol{r}_j - \boldsymbol{r}_i$, where $\boldsymbol{r}_j$ and $\boldsymbol{r}_i$ are the locations of the TLS and the chromophore. $\Delta\rho_j = (\rho_j)_{11} - (\rho_j)_{00}$, where $(\rho_j)_{11}$ and $(\rho_j)_{00}$ are the excited state and the ground state populations of the TLS, respectively. In writing this equation, we have implicitly assumed that the behavior of the TLS is not affected by the chromophores [20]. In addition, we have ignored the off-diagonal interactions. These interactions are in the form of couplings between the chromophore's electronic eigenstates. Because the energy separations of the eigenstates are usually, and as assumed in our case, much larger than the energy separations of the TLS, the effect of the interactions appears to be a far off-resonance E field. Therefore, the off-diagonal interactions should not contribute significantly to the dephasing process [13–15]. The third term in H_0 describes population relaxation of the excited chromophore by radiative and nonradiative decay and other standard dephasing processes such as excited state–acoustic phonon coupling [23,24]. At very low temperatures ($T < 4$ K), only dephasing arising from TLS has been observed in glasses. At somewhat higher temperature, dephasing from pseudo-local modes has been reported [8]. This third term in the Hamiltonian will not be considered explicitly. Rather, a phenomenological decay term for population relaxation and any non-TLS dephasing will be added at the appropriate point.

The semiclassical interaction Hamiltonian,

$$H_{\text{int}} = -\boldsymbol{\mu}_i \cdot \boldsymbol{E}(\boldsymbol{r}_i, t) ,$$

describes the interaction between the laser field and the chromophore. $\boldsymbol{\mu}_i$ is the transition dipole moment and $\boldsymbol{r}_i$ the location of the chromophore.

In a general four-wave-mixing experiment, the laser field consists of three input beams,

$$\boldsymbol{E}(\boldsymbol{r}, t) = \sum_{j=1}^{3} \boldsymbol{E}_j(t) \exp[\mathrm{i}(\boldsymbol{k}_j \cdot \boldsymbol{r} - \omega_j t)] + \text{c.c.} \tag{2.2}$$

The experimental observable, the intensity of the output beam, is the square of the absolute value of the induced

macroscopic nonlinear polarization that acts as the source in Maxwell's equations. The polarization is given by

$$\mathscr{P}(r,t)=\frac{1}{V}\sum_i \mathrm{Tr}\{\mu_i\rho_i(t)\}=\rho_c\langle P(r_i,t)\rangle\,,$$

$$P(r_i,t)=\mathrm{Tr}\{\mu_i\rho_i(t)\}=[\mu_i]_{ab}[\rho_i(t)]_{ba}+[\mu_i]_{ba}[\rho_i(t)]_{ab}\,. \tag{2.3}$$

ρ_i is the density matrix of the ith chromophore. ρ_c is the density of the chromophores. $\langle\ \rangle$ denotes an average over the chromophores, which is performed over the spread of transition frequency detunings, the spatial distribution, and the projection of the E field onto the random directions of the chromophores' transition dipole moment directions. The averages are performed over a volume, V, which is chosen to be macroscopically small, $|\boldsymbol{k}\cdot(\boldsymbol{r}_i-\boldsymbol{r})|\ll 1$, so that the phase factor inside the average can be taken out, $\exp(\mathrm{i}\boldsymbol{k}\cdot\boldsymbol{r}_i)\approx\exp(\mathrm{i}\boldsymbol{k}\cdot\boldsymbol{r})$, but microscopically large enough to include a significant number of chromophores.

To the third order in the input field strength, the general form of the polarization can be expressed [25] as

$$P(r_i,t)=\sum_{k_s,\omega_s} P_i(\boldsymbol{k}_s,t)\exp[\mathrm{i}(\boldsymbol{k}_s\cdot\boldsymbol{r}_i-\omega_s t)]\,, \tag{2.4}$$

where $\boldsymbol{k}_s$ and ω_s are the appropriate combinations of input laser beam wavevectors and frequencies for the particular nonlinear experiment under consideration. In typical echo experiments, the frequencies of the laser fields are degenerate and resonant with one of the transitions of the chromophore, $\omega_1=\omega_2=\omega_3=\omega$, and the signal is detected along a direction $\boldsymbol{k}_s=-\boldsymbol{k}_1+\boldsymbol{k}_2+\boldsymbol{k}_3$. Under these conditions, the nonlinear polarization that generates the echo signal is

$$P(r_i,t)=P_i(\boldsymbol{k}_s,t)\exp[\mathrm{i}(\boldsymbol{k}_s\cdot\boldsymbol{r}_i-\omega t)]+\mathrm{c.c.}\,,$$

$$P_i(\boldsymbol{k}_s,t)=-\mathrm{i}\int_0^\infty \mathrm{d}t_1\int_0^\infty \mathrm{d}t_2\int_0^\infty \mathrm{d}t_3\, R_i(t_3,t_2,t_1)$$

$$\times\exp[\mathrm{i}\omega(t_1-t_3)]\times E_1^*(t-t_3-t_2-t_1)\,E_2(t-t_3-t_2)\,E_3(t-t_3)\,, \tag{2.5}$$

where R_i is the nonlinear response function of the chromophore, which is defined as a matrix element in Liouville space [25] and contains the necessary information about the chromophore–glass system.

2.2. The four-point correlation response function

The chromophore is modeled as having three levels. Level a represents the ground electronic state of the chromophore and level b the excited electronic state which is coupled to the ground state by the radiation field. Level b decays to levels a and c with rates γ_{ba} and γ_{bc}, respectively. Its total decay rate is $\gamma_b=\gamma_{ba}+\gamma_{bc}$. Level c is a triplet or other transient intermediate state which decays to the ground state at a rate γ_{ca}. Optical transitions only occur between levels a and b. The transition frequency of the chromophore outside the glassy matrix is $\omega_{ab}=\omega$. The matrix causes a shift in the transition frequency, $\Delta\omega(t)$, that can be split into two parts, $\Delta\omega(t)=\Delta(s)+\Delta(t)$. The detuning $\Delta(s)$ results from a set of coordinates S that are static on all relevant time scales and can be treated as inhomogeneous broadening of the system. The time-dependent detuning $\Delta(t)$, however, is caused by a set of coordinates D that fluctuate within the time scale of the experiment. In the problem considered here, D is an ensemble of TLS.

With this model, the nonlinear response function can be calculated [25,8] (see appendix A),

$$R_i(t_3,t_2,t_1)=\mu_i^4\exp\{\mathrm{i}[\omega_{ab}+\Delta_i(s)](t_1-t_3)-\gamma(t_1+t_3)/2\}A(t_2)C_i(t_3,t_2,t_1)\,, \tag{2.6}$$

$$A(t_2)=2\exp(-\gamma_b t_2)+\phi_c[\exp(-\gamma_{ca}t_2)-\exp(-\gamma_b t_2)]\,, \tag{2.6'}$$

$$C_i(t_3, t_2, t_1) = \exp\left(-\mathrm{i} \int_{t_2+t_1}^{t_3+t_2+t_1} \Delta_i(t')\, \mathrm{d}t' + \mathrm{i} \int_0^{t_1} \Delta_i(t')\, \mathrm{d}t' \right),$$

where $\gamma/2 = \gamma_b/2 + \Gamma'$, Γ' accounts for dephasing from processes other than coupling to the TLS. As discussed in connection with eq. (2.1), in glasses at low temperature, only TLS-induced dephasing has been observed. In this case, $\Gamma' = 0$. $\phi_c = \gamma_{bc}/\gamma_b$ is the triplet yield, and μ_i is now the component of the transition dipole moment along the direction of polarization of the E field. The units are chosen such that Planck's constant, $\hbar$, is equal to unity.

After an average over the inhomogeneously broadened transition frequency distribution (this is actually part of the average over i), eq. (2.6) becomes

$$R_i(t_3, t_2, t_1) = \mu_i^4 \rho_1 \exp(-\gamma t_1) A(t_2)\, C_i(t_1, t_2, t_1)\, \delta(t_3 - t_1) = R_i(t_1, t_2)\, \delta(t_3 - t_1)\,. \tag{2.7}$$

Here we have used the fact that the inhomogeneous absorption lines in glasses are usually extremely broad, so that the chromophores are uniformly distributed with a density ρ_1 over the laser frequency bandwidth.

Substituting eq. (2.7) into eqs. (2.5) and (2.3), and integrating over t_3, we have

$$\mathscr{P}(\boldsymbol{r}, t) = \rho_c \langle P(\boldsymbol{r}_i, t) \rangle = -\mathrm{i}\rho_c \rho_1 \exp(-\mathrm{i}\omega t) \int_0^\infty \mathrm{d}t_1 \int_0^\infty \mathrm{d}t_2 \exp(-\gamma t_1)\, A(t_2)\, F(t_1, t_2)$$

$$\times E_1^*(t - t_2 - 2t_1)\, E_2(t - t_2 - t_1)\, E_3(t - t_1) + \text{c.c.}\,, \tag{2.8}$$

$$F(t_1, t_2) = \langle \mu_i^4 \exp(\mathrm{i}\boldsymbol{k}_s \cdot \boldsymbol{r}_i)\, C_i(t_1, t_2, t_1) \rangle\,. \tag{2.8'}$$

Part of the average in eq. (2.8') involves the random projections of the chromophores' transition dipole moments onto the direction of polarization of the E field. Since it is independent from other random variables, we can perform this average separately. Denoting $\langle \mu_i^4 \rangle$ by μ^4, we have

$$F(t_1, t_2) = \mu^4 \langle \exp(\mathrm{i}\boldsymbol{k}_s \cdot \boldsymbol{r}_i)\, C_i(t_1, t_2, t_1) \rangle\,. \tag{2.9}$$

As discussed above, the averaging volume is restricted to a dimension much smaller than the field wavelength. The phase factor inside the average can then be taken out

$$\langle \exp(\mathrm{i}\boldsymbol{k}_s \cdot \boldsymbol{r}_i)\, C_i(t_1, t_2, t_1) \rangle = \exp(\mathrm{i}\boldsymbol{k}_s \cdot \boldsymbol{r}) \langle C_i(t_1, t_2, t_1) \rangle\,.$$

Thus the final expression for the macroscopic polarization is

$$\mathscr{P}(\boldsymbol{r}, t) = -\mathrm{i}\rho_c \rho_1 \mu^4 \exp[\mathrm{i}(\boldsymbol{k}_s \cdot \boldsymbol{r} - \omega t)] \int_0^\infty \mathrm{d}t_1 \int_0^\infty \mathrm{d}t_2 \exp(-\gamma t_1)\, A(t_2)$$

$$\times C(t_1, t_2, t_1)\, E_1^*(t - t_2 - 2t_1)\, E_2(t - t_2 - t_1)\, E_3(t - t_1) + \text{c.c.}\,, \tag{2.10}$$

where

$$C(t_1, t_2, t_1) = \langle C_i(t_1, t_2, t_1) \rangle\,,$$

is a special case of the four-point correlation function defined in ref. [25]. Eq. (2.10) is a general result for all types of photon echo experiments which have the phase matching scheme described above and where the environmental perturbations can be described by time-dependent frequency modulations. The actual form of the four-point correlation function, $C(t_1, t_2, t_1)$, has to be derived through a detailed analysis of the time-dependent perturbations.

To illustrate the significance of the four-point correlation function, we consider a stimulated photon echo. Let $E_1(t) = E(t)$, $E_2(t) = E(t - \tau)$, and $E_3(t) = E(t - \tau - T_w)$, where

$$E(t)=\delta(t)\,\theta/2\mu\,,\quad \theta=2\mu\int_{0-}^{0+}\mathrm{d}t\,E(t)\,,$$

and $|\theta|$ is the laser pulse flip angle (pulse area). Then eq. (2.10) becomes

$$\mathscr{P}(r,t)=-\mathrm{i}\rho_c\rho_1\mu(|\theta|^2\theta/8)\exp[\mathrm{i}(k_s\cdot r-\omega t)]\,\delta(t-2\tau-T_W)\exp(-\gamma\tau)\,A(T_W)\,C(\tau,T_W,\tau)+\text{c.c.}\qquad(2.11)$$

From eq. (2.11), we see that the four-point correlation function, $C(t_1, t_2, t_1)$, describes the dephasing of a stimulated photon echo caused by fluctuations of the TLS in the glass. In the absence of TLS fluctuations, $C(t_1, t_2, t_1)$ is equal to unity, and the decay arises only from population relaxation and conventional phonon dephasing processes. The three times in the argument of the correlation function are actually the three time intervals between the four pulses in a stimulated echo. Here the first t_1 corresponds to the time delay, τ, between the second and the first pulses and t_2 the time delay, T_W, between the third and the second pulses. The second t_1 is the time delay between the echo signal pulse and the third applied pulse of the stimulated echo sequence. The limit $t_2=0$ gives the two-pulse photon echo correlation function, i.e. the two-pulse photon echo is equivalent to a stimulated echo with the second and third pulses coincident in time.

The physical meaning of the function $A(t_2)$ in eq. (2.6′) also becomes clear. It describes how the echo signal is affected by population decays during the waiting time period, T_W. The longest waiting time is determined by either the triplet state lifetime, $1/\gamma_{ca}$, or the excited state lifetime, $1/\gamma_b$, whichever is longer. In most cases, $1/\gamma_{ca}\gg 1/\gamma_b$, the triplet state acts like a bottleneck, and the longest waiting time is given by $1/\gamma_{ca}$. Thus we can define $1/\gamma_{ca}$ as the sample's "memory time". In the absence of a triplet bottleneck or other bottleneck state, the sample's memory time is given by $1/\gamma_b$.

3. Evaluation of the correlation function using the TLS model

In refs. [14,15] a method for calculating the correlation function

$$C(t_1,t_2,t_1)=\langle C_i(t_1,t_2,t_1)\rangle$$

is developed to study dephasing in spin echo experiments. We will follow a similar route in our discussion [8,20,21]. To start, we write

$$C(t_1,t_2,t_1)=\langle\exp[-\mathrm{i}\varphi_i(t_1,t_2)]\rangle\,,\qquad(3.1)$$

$$\varphi_i(t_1,t_2)=\sum_j^N\varphi_{ij}(t_1,t_2)\,,\quad \varphi_{ij}(t_1,t_2)=\int_{t_2+t_1}^{t_2+2t_1}\Delta_{ij}(t')\,\mathrm{d}t'-\int_0^{t_1}\Delta_{ij}(t')\,\mathrm{d}t'\,.$$

i and j label respectively a chromophore and a TLS.

3.1. Average over the history of the frequency perturbation

φ_i results from perturbations by a large number of fluctuating TLS. Each chromophore is associated with a different φ_i. Thus φ_i has to be treated as a random variable. Following ref. [26], we assume that dominant part of φ_i is induced by a number ($\geqslant 10$) of nearby *independent* TLS, so that φ_i is approximately described by a Gaussian distribution. Alternatively, one can say that the time-dependent frequency detuning, $\Delta_{ij}(t')$, undergoes a random process and has to be averaged over all the possible path histories. The summation of the $\Delta_{ij}(t')$, $\Delta_i(t')$, obeys a Gaussian distribution. Since $\varphi_i(t_1, t_2)$ is a linear combination of $\Delta_i(t')$, it will also obey a Gaussian distribution. Thus the ensemble average of φ_i is equivalent to an average of the path history of $\Delta_i(t')$.

However, it should be pointed out that the Gaussian phase distribution is a less restricted condition, for even if $\Delta_i(t')$ is not Gaussian, φ_i can still approximated by a Gaussian variable, provided the random frequency modulation is fast compared to the experiment.

Averaging over the path histories, we have

$$\langle \exp[-i\varphi_i(t_1, t_2)] \rangle_H = \exp[-i\langle \varphi_i(t_1, t_2) \rangle_H - \sigma^2(\varphi_i)/2] , \tag{3.2}$$

where σ is the deviation of the distribution,

$$\sigma^2(X) = \langle (\delta X)^2 \rangle = \langle (X - \langle X \rangle)^2 \rangle . \tag{3.3}$$

It is straightforward to how that $\langle \varphi_i(t_1, t_2) \rangle \equiv 0$, and that

$$\sigma^2(\varphi_i) = \sum_{j,j'}^{N} \langle \delta\varphi_{ij} \delta\varphi_{ij'} \rangle_H = \sum_{j}^{N} \sigma^2(\varphi_{ij}) . \tag{3.4}$$

We should point out here that after eq. (3.2), the subindex is used solely as a reference to the positions of the chromophores.

Besides an average over the path histories, the correlation function also has to be averaged over the random distributions of parameters which describe the TLS. Each individual TLS has a location, $\boldsymbol{r}_j$, and some internal parameters, which are treated as random variables. In the standard TLS model [1–4], these internal parameters are the TLS energy splitting E, and the tunneling parameter $\lambda = d(2MV/\hbar)^{1/2}$. d is the distance of the tunneling motion, M is the reduced mass of the tunneling particles, and V is the height of the TLS potential barrier. As a result, eq. (3.1) becomes

$$C(t_1, t_2, t_1) = \langle C_i(t_1, t_2, t_1) \rangle_{H,TLS} = \left\langle \prod_{j}^{N} \exp[-\sigma^2(\varphi_{ij})/2] \right\rangle_{TLS}$$

$$= \prod_{j}^{N} \langle \exp[-\sigma^2(\varphi_{ij})/2] \rangle_{E_j, \lambda_j, r_{ij}} = \langle \exp[-\sigma^2(\varphi_{ij})/2] \rangle^{N}_{E_j, \lambda_j, r_{ij}} , \tag{3.5}$$

where $\boldsymbol{r}_{ij} = \boldsymbol{r}_i - \boldsymbol{r}_j$, and

$$\langle \rangle_{r_{ij}} = (1/V) \int_0^\infty d\boldsymbol{r}_{ij} .$$

In deriving eq. (3.5), we have assumed that both the TLS and the chromophores are uniformly distributed over the averaging volume, V, so that all the TLS and the chromophores can be treated identically. Omitting the indices and invoking the relation

$$\lim_{N \to \infty} (1 + x/N)^N = \exp(x)$$

we can rewrite eq. (3.5) as

$$C(t_1, t_2, t_1) = \exp\{-N\langle 1 - \exp[-\sigma^2(\varphi)/2] \rangle_{E,\lambda,r}\} . \tag{3.6}$$

We note that now the averages are over the possible energy separations and tunneling parameters of a single TLS, and over the random distribution of possible distances between the TLS and an arbitrary chromophore.

The variance of the phase perturbation by the TLS is calculated in appendix B. As a result, eq. (3.6) can be explicitly written as

$$C(t_1, t_2, t_1) = \exp\{-N\langle 1 - \exp\{-[\sigma(\Delta)\, t_1 f(Rt_1, Rt_2)]^2\} \rangle_{E,\lambda,r}\} , \tag{3.7}$$

$$f(Rt_1, Rt_2) = (\sqrt{2}/Rt_1)\{\exp(-Rt_1) - (1 - Rt_1) - \exp[-R(t_2 + t_1)][\cosh(Rt_1) - 1]\}^{1/2} ,$$

$\sigma(\Delta) = \operatorname{sech}(E/2kT)\,\Delta_0$,

where Δ_0 is the amplitude of the frequency perturbation induced by the TLS,

$\Delta_0(E, \lambda, r) = \xi_b - \xi_a$.

ξ_b and ξ_a are defined in eq. (2.1′).

3.2. Averages over the spatial distribution and the internal parameters of the TLS

Theoretical analysis of photon echo experiments and optical hole burning experiments in glasses, which yield exponential decays and Lorentzian lines, respectively, demonstrates that the amplitude of the perturbation of a chromophore induced by a single fluctuating TLS is proportional to the cube of the inverse of the distance between the chromophore and the TLS [1,8,20]. This is consistent with either a strain dipole [18] or an electric dipole coupling mechanism. Letting $\Delta_0 = \eta/r^3$, we can perform the average over the random spatial distribution of the TLS. Eq. (3.7) then becomes

$$C(t_1, t_2, t_1) = \exp\{-\alpha t_1 \langle \eta \operatorname{sech}(E/2kT)\, f(Rt_1, Rt_2)\rangle_{E\lambda}\}, \tag{3.8}$$

$\alpha = \frac{4}{3}\pi^{3/2}\rho_G$,

where $\rho_G = N/V$ is the density of TLS, and R is the relaxation rate of the TLS towards equilibrium, which is a function of E and λ, and has a very broad range of values.

In deriving eq. (3.8), we have used the relation

$$\int_0^\infty \mathrm{d}x\, [1-\exp(-x^2)]/x^2 = \pi^{1/2}.$$

It should be pointed out that by letting the lower limit of this integral be 0, we have implicitly assumed

$t_1 \eta \operatorname{sech}(E/2kT)\, f(Rt_1, Rt_2) \ll V$,

i.e. the TLS outside of the averaging volume do not contribute to the dephasing of the chromophore under investigation. From eq. (3.4), we see that the term responsible for the dephasing is in the form of

$$\sum_j^N \sigma^2(\varphi_{ij}) \propto \int \mathrm{d}r\, r^2 (1/r^6).$$

The dephasing induced by the TLS decreases quickly as the distance between the TLS and the chromophore increases. This argument is also consistent with the fact that our averaging volume is much smaller than the laser wavelength.

To perform the averages over E and λ, we assume the following. (a) The constant describing the coupling between the TLS and the chromophore is given by [1],

$\eta = F\delta/E$,

where δ is the asymmetry of the double potential wells of the TLS. With the standard TLS model, it is quite straightforward to show that this relation is consistent with a dipolar coupling mechanism. (b) The fluctuations of the TLS are only caused by resonant single phonon assisted tunneling processes [1–4]. Assuming the Debye approximation can be used to describe the density of states of the phonons, one finds the relaxation rate of the TLS (see, for example, ref. [17]) is

$R = \Omega\delta_0^2 E \coth(E/2kT)$,

where Ω is a collection of constants describing the coupling of the TLS to the acoustic phonons of the glass, and δ_0 is the coupling between the double potential wells of the TLS, $\delta_0 \propto e^{-\lambda}$. We note that the relaxation rate R is often incorrectly assumed (see, for example, refs. [1,8]) to be the average of the up and down transition rates of the TLS. In fact, it is the *sum, not the average*, of the up and down transition rates of the TLS.

The common assumption about distributions of TLS in glasses is that $P(\delta, \lambda) = \langle P \rangle$ is a constant in the range of δ and λ of interest in a study [1–4]. Recalling the relation $E = (\delta^2 + \delta_0^2)^{1/2}$, we can transform this constant distribution of δ and λ into a distribution of E and R,

$$P(\delta, \lambda)\, \mathrm{d}\delta \mathrm{d}\lambda = P(E, R)\, \mathrm{d}E \mathrm{d}R = \tfrac{1}{2} \langle P \rangle R^{-1} (1 - R/R_{\max}(E))^{-1/2}\, \mathrm{d}E \mathrm{d}R\,,$$

where E and R are in the ranges of $(\delta_{0,\min}, E_{\max})$ and $[R_{\min}(E), R_{\max}(E)]$, respectively. The cutoffs, $\delta_{0,\min}$ and $E_{\max}$, are introduced to keep the total number of states of the TLS from diverging, and the relaxation rate limits are defined as

$$R_{\min}(E) = \Omega \delta_{0,\min}^2 E \coth(E/2kT)\,, \quad R_{\max}(E) = \Omega E^3 \coth(E/2kT)\,.$$

An extension of this model is to let $\langle P \rangle$ vary slightly with E, i.e. $\langle P \rangle = P_0 E^{\mu}$ between $E_{\max} \geqslant E \geqslant E_{\min} \equiv \delta_{0,\min}$ [1]. With this model, we can rewrite the average in eq. (3.8) as

$$\langle \eta \operatorname{sech}(E/2kT) f(Rt_1, Rt_2) \rangle_{E\lambda} = F \int_{E_{\min}}^{E_{\max}} \mathrm{d}E\, P_0 E^{\mu} \operatorname{sech}(E/2kT) \int_{R_{\min}}^{R_{\max}} \mathrm{d}R\, f(Rt_1, Rt_2)/2R\,, \tag{3.9}$$

where we have used the identity $\delta/E = [1 - R/R_{\max}(E)]^{-1/2}$. We see from this equation that while the energies of the TLS belong to a broad distribution, the relaxation rates of the TLS with a given energy are also distributed over a broad range. Noting that the dominant part of the integral over E is within $E \leqslant 2kT$ and that $R_{\min}(E)$ is insensitive to E in this range, we can replace the limits in the integral over R by

$$R_{\min}(E) \to 2kT\Omega\delta_{0,\min}^2\,, \quad R_{\max}(E) \to 2kT\Omega E^2\,. \tag{3.9'}$$

Using these new integral limits, we can easily interchange the order of the integrals. Eq. (3.8) then becomes

$$C(t_1, t_2, t_1) = \exp\left(-t_1 \int_{R_{\min}}^{R_{\max}(E_{\max})} \mathrm{d}R\, \beta(R) f(Rt_1, Rt_2)/R \right) \equiv \exp[-t_1 \langle f(Rt_1, Rt_2) \rangle_R]\,, \tag{3.10}$$

$$\beta(R) = \alpha(F/2)(kT)^{1+\mu} P_0 \int_{x_{\min}}^{x_{\max}} \mathrm{d}x\, x^{\mu} \operatorname{sech}(x/2)\,, \tag{3.10'}$$

where $x = E/kT$, $x_{\min} = 2[R/R_{\max}(2kT)]^{1/2}$, and $x_{\max} = E_{\max}/kT$.

We note that eq. (3.10) reflects a general feature of optical dephasing in the presence of spectral diffusion. Since $f(Rt_1, Rt_2)$ is essentially a constant between $R = (t_2 + t_1)^{-1}$ and $R = t_1^{-1}$ (see appendix C), all fluctuations whose rates fall into this range contribute to the dephasing. For different types of physical systems, the fluctuation rate distributions can vary, and the dephasing rate may be related to the average in a different manner. It remains true, however, that the total optical dephasing rate is governed by a summation over a fluctuation rate distribution with a weight function slowly varying in the range of $((t_2 + t_1)^{-1}, t_1^{-1})$.

$E_{\max}$ is usually considered to be determined by the glass transition temperature, i.e. $E_{\max} = kT_g$. In most optical dephasing experiments, we have $T \ll T_g$. The upper limit of the integral in eq. (3.10') can thus be set to infinity. The lower limit of the integral is generally a function of R. However, if the relaxation rates of interest satisfy the condition $R \ll R_{\max}(2kT)$, this lower limit can be set to zero. As a result, we find that in the range of $R_{\min} < R \ll R_{\max}(2kT)$ $\beta(R)$ is independent of R, and therefore the relaxation rate distribution function is proportional to $1/R$. Since $f(Rt_1, Rt_2)$ falls to zero very quickly at $Rt_1 \geqslant 1$ (see appendix C), we can restate our

conclusion as: the relaxation rate distribution function is given by $1/R$ only if $R_{max}(2kT) \gg 1/t_1$. Physically, this means that if the dominant part of the optical dephasing is induced by those TLS whose energy separations fall in the range of $[E_{min}/(R_{min}t_1), 2kT]$, the relaxation distribution function will appear to be proportional to $1/R$ in the range of $(R_{min}, 1/t_1)$. It has been determined that in fused silica glass, $R_{max}(2kT)$ is on the order of 10^{10} Hz at $T \approx 2$ K [18]. Experimental data shows that the $1/R$ behavior of the distribution function extends to $t_1 \approx 10$ ps in some organic glasses [8], indicating a $R_{max}(2kT)$ on the order of $\geqslant 10^{12}$ Hz. This seems reasonable because R is inversely proportional to the fifth power of the velocity of the sound [18], which is slower in the softer organic glasses.

Since the distribution function is a constant in the $\ln(R)$ scale, we can evaluate the integral over R simply by examining the behavior of the function $f(Rt_1, Rt_2)$ in this scale. For $t_2 = 0$, $C(t_1, 0, t_1)$ describes the dephasing of the two-pulse photon echo. In this case $f(Rt_1, 0)$ is a narrowly peaked function centered about $\ln(Rt_1) = 0$. Analysis of experimental results [8,22] suggests that the lower limit of the integral, R_{min}, is less than 10^5 Hz. In a typical system, the time scale measured by a two-pulse photon echo is in the range of picoseconds to nanoseconds. Thus the entire peak of $f(Rt_1, 0)$ lies within the range (R_{min}, R_{max}). We can safely change the integral limits to $(0, \infty)$ and perform the integration. As a result, the two-pulse photon echo correlation function becomes an exponentially decaying function,

$$C(t_1, 0, t_1) = \exp(-\beta\Theta t_1) , \tag{3.11}$$

$$\Theta = \int_0^\infty dx f(x, 0)/x \approx 3.6 .$$

Experimentally, it is found that two-pulse photon echo signal decays exponentially in the glasses that have been studied [8,20]. This indicates that in these systems, the relaxation distribution function is indeed in the form of $1/R$ for $R \gg R_{min}$, which is consistent with our earlier discussions.

In general, we can write

$$C(t_1, t_2, t_1) = C(t_1, 0, t_1)\, C_1(t_1, t_2, t_1) = \exp(-\beta\Theta t_1)\, C_1(t_1, t_2, t_1) , \tag{3.12}$$

where C_1 is the correlation function which describes the dephasing arising from spectral diffusion [8]. To a good approximation, the function $f(Rt_1, Rt_2) - f(Rt_1, 0)$ can be replaced by a step function (see appendix C),

$$f(Rt_1, Rt_2) - f(Rt_1, 0) \approx H[R - B_1/(t_1 + t_2)]H(B_1/t_1 - R) , \tag{3.13}$$

where B_1 is a constant of order of unity. Using this approximation and assuming that $R_{max} > 1/t_1$, we can carry out the integral in eq. (3.10) with limits $(0, \infty)$. The correlation function C_1 then becomes

$$C_1(t_1, t_2, t_1) \approx \exp[-\beta t_1 \ln(t_c/t_1)] , \tag{3.14}$$

$$t_c = \min(t_1 + t_2, 1/R_{min}) .$$

Thus the final expression for the four-point correlation function becomes

$$C(t_1, t_2, t_1) = \exp[-\beta t_1(\Theta + \ln(t_c/t_1)] . \tag{3.15}$$

It should be pointed out that our choice of using a Gaussian stochastic process to evaluate the four-point correlation function is mainly for mathematical simplicity. The real process is probably better described by a "sudden jump" model [15]. The actual form of the weight function $f(Rt_1, Rt_2)$ derived using this model differs from that derived here. In particular, the sudden jump model predicts that $f(Rt_1, Rt_2)$ falls to zero at a faster rate at the edge $R(t_2 + t_1) < 1$ [14,15]. Except for this, the overall behaviors of the weight functions derived from these two models are very similar [15]. This is because of two reasons. For $Rt_1 \gg 1$, the TLS can flip many times during the time intervals $[0, t_1]$ and $[t_1 + t_2, 2t_1 + t_2]$, making the accumulated phase errors converge to a Gaussian distribution. For $Rt_2 \gg 1$, the Markoffian process, which itself is a result of the sudden jumps between

the two levels (see appendix B), ensures that the total phase error is independent of t_2. As a result, the weight function is flat in the region $1/\tau > R > 1/T_W$. If the distribution function of the relaxation rate were a δ function, $\delta(R-W)$, as assumed in refs. [14,15], and $W(t_2+t_1)<1$, these two models would yield different results. However, as seen from our discussion, the distribution function spans a very wide range, and it is the integral of $f(Rt_1, Rt_2)$ that counts. The error introduced by different falling edges is negligible. This is also consistent with the step function approximation used in eq. (3.13).

4. Application to accumulated grating echo experiments

In this section, we apply our results to the accumulated grating echo experiment. To simplify the notation, we rewrite eq. (2.11) as

$$\mathscr{P}(r,t)=P(k_s,t)\exp[i(k_s\cdot r-\omega t)]+\text{c.c.}, \tag{4.1}$$

$$P(k_s,t)=-i\int_0^\infty dt_1\int_0^\infty dt_2\, R(t_1,t_2)\,E_1^*(t-t_2-2t_1)\,E_2(t-t_2-t_1)\,E_3(t-t_1)\,,$$

$$R(t_1,t_2)=\rho_c\rho_1\mu^4\exp(-\gamma t_1)\,A(t_2)\,C(t_1,t_2,t_1)\,.$$

Only unsaturated accumulated grating echoes will be considered. This is consistent with our perturbative calculation of the nonlinear polarization.

4.1. Conventional accumulated grating echoes

Consider a common configuration of the accumulated grating echo experiment. A cw mode-locked laser beam, consisting of a stream of pulses typically separated by about 10 ns, is split into two beams which are subsequently crossed in the sample. The second beam is delayed from the first by a time interval, τ, so that $E_1(t)=E(t)$, $E_2(t)=E_3(t)=E(t-\tau)$, and $k_3=k_2\neq k_1$. Under these conditions, the echo polarization becomes

$$P(k_s,t;\tau)=-i\int_0^\infty dt_1\int_0^\infty dt_2\, R(t_1,t_2)\,E^*(t-t_2-2t_1)\,E(t-t_2-t_1-\tau)\,E(t-t_1-\tau)\,. \tag{4.2}$$

The laser pulse duration is usually much shorter than the time delay, τ, and the optical dephasing time. Thus we can write

$$E(t)=\sum_{n=0}^{\infty}\delta(t-nT_R)\theta/2\mu\,, \tag{4.3}$$

where T_R is the repetition time and $|\theta|$ is the flip angle of the laser pulse. Eq. (4.2) then becomes

$$P(k_s,t;\tau)=-i\frac{|\theta|^2\theta}{8\mu^3}\sum_{n_1\leqslant n_2,n_3}R((n_2-n_1)T_R+\tau,(n_3-n_2)T_R)\,\delta(t-(n_3+n_2-n_1)T_R-2\tau)\,, \tag{4.4}$$

where n_j correspond to $E_j(t)$, $j=1,2,3$.

An echo signal occurs after each pulse pair. After the Nth pulse pair, the time of occurrence of the echo signal is given by

$$P(k_s,t;\tau)\propto\delta(t-NT_R-2\tau)\,.$$

Using the substitution

$$\delta(t-(n_3+n_2-n_1)T_R-2\tau)\rightarrow\delta(t-NT_R-2\tau)\,\delta_{n_3+n_2-n_1,N}\,,$$

we rewrite eq. (4.4) as

$$P(\boldsymbol{k}_s,t;\tau)=-i\frac{|\theta|^2\theta}{8\mu^3}\sum_{\Delta n,n_3}^{N}R((N-n_3)T_R+\tau,\Delta n_2 T_R)\delta(t-NT_R-2\tau)\,, \tag{4.5}$$

where $\Delta n=n_3-n_2$.

If the dephasing time of the sample, T_{dp}, is much shorter than laser pulse repetition time, then

$$P(\boldsymbol{k}_s,t;\tau)=-i\frac{|\theta|^2\theta}{8\mu^3}\sum_{\Delta n}^{N}R(\tau,\Delta n_2 T_R)\delta(t-NT_R-2\tau)$$

$$=-i\rho_c\rho_1\mu(|\theta|^2\theta/8)\,\delta(t-NT_R-2\tau)\exp(-\gamma\tau)\sum_{\Delta n}^{N}A(\Delta n_2 T_R)\,C(\tau,\Delta n_2 T_R,\tau)\,. \tag{4.6}$$

Letting $N\rightarrow\infty$ gives the steady state value of the echo polarization. In those systems in which the echo signal accumulates, $A(\Delta nT_R)$ and $C(\tau,\Delta nT_R,\tau)$ are slowly varying functions compared with T_R. Thus we can replace the summation by an integral and rewrite eq. (4.6) as

$$\mathscr{P}(\boldsymbol{k}_s,t;\tau)=-i\rho_c\rho_1\mu(|\theta|^2\theta/8)\,\delta(t-NT_R-2\tau)\exp(-\gamma\tau)\,T_R^{-1}\int_0^{NT_R}dt_2\,A(t_2)\,C(\tau,t_2,\tau)\,. \tag{4.7}$$

The physical interpretation of eq. (4.7) is straightforward: the accumulated photon echo is the sum of a series of stimulated photon echoes with a constant $t_{21}=\tau$, and variable t_{32}, $0<t_{32}<t_{max}$, where t_{max} is given either by NT_R or by the memory time of the sample.

We note that in the absence of TLS-induced fluctuations, the four-point correlation function derived here is equal to unity. Eq. (4.6) then yields identical results as those given in ref. [7]. Only in this case, i.e. in systems without spectral diffusion arising from TLS or other mechanisms, will the accumulated grating echo measure the same dephasing time as the two-pulse photon echo.

In those cases where the condition $T_{dp}\ll T_R$ is not satisfied, one will have to calculate the double summation in eq. (4.5). However, if there is a phase fluctuation between the pulse pairs, there will be an extra phase factor, $\exp[i(\phi_{n_3}+\phi_{n_2}-\phi_{n_1})]$, in eq. (4.4). When the phase fluctuations are so large that the pulse pairs are completely uncorrelated, the ensemble average of the phase fluctuations will force $n_1=n_2$, which leads to an identical result as eq. (4.6). As will be seen below, this is exactly the case which occurs if one uses a broad band incoherent light source rather than the mode-locked laser discussed in this section.

4.2. Accumulated photon echoes using incoherent light sources

Consider an incoherent photon echo experiment with the same beam configuration as that discussed above. Thus we can start from eq. (4.2). In order to resolve the optical dephasing of the sample, one has to make the laser field a much faster varying function of time than the response function so that

$$|R/\tau_c|\gg|dR(t_1,t_2)/dt_2|,\ |dR(t_1,t_2)/dt_1|\,,$$

where τ_c is the correlation time of the laser field. This relation implies $|dE(t_2)/(E\,dt_2)|\gg|dR(t_1,t_2)/(R\,dt_2)|$. Thus we can write the integral over t_2 as

$$\int_0^\infty dt_2\, R(t_1, t_2)\, E^*(t-t_2-2t_1)\, E(t-t_2-t_1-\tau) = \sum_{n=0}^{\infty} R(t_1, n\Delta t_2) \int_{n\Delta t_2}^{(n+1)\Delta t_2} dt_2\, E^*(t-t_2-2t_1)\, E(t-t_2-t_1-\tau)$$

$$= \sum_{n=0}^{\infty} \Delta t_2\, R(t_1, n\Delta t_2) \langle E^*(t-t_2-2t_1)\, E(t-t_2-t_1-\tau)\rangle_{\Delta t_2}\,, \tag{4.8}$$

where $\langle\ \rangle$ denotes an average over a time interval, Δt_2. The time interval is chosen in such a way that: (a) it is small enough that $R(t_1, t_2)$ does not vary much within the time interval; and (b) it is much larger than the correlation time of the laser field, τ_c. The second requirement allows us, according to the ergodic theorem, to replace the time average by an ensemble average,

$$\langle E^*(t-t_2-2t_1)\, E(t-t_2-t_1-\tau)\rangle_{\Delta t_2} = \langle E^*(t-t_2-2t_1)\, E(t-t_2-t_1-\tau)\rangle_{\text{ensemble}}$$

$$= g(t_1-\tau)\langle |E(t-t_2-2t_1)|^2\rangle_{\text{ensemble}}\,, \tag{4.9}$$

where g is the first-order correlation function of the laser field and $\langle |E(t-t_2-2t_1)|^2\rangle$ is the slowly varying laser intensity envelope. Experimentally, the measurement is usually repeated many times. The second requirement is then relaxed to $\Delta t_2 > \tau_c$, and $N \gg 1$, where N is the total number of measurements. In a transient experiment, where the laser pulse duration is much shorter than the memory time, N is the total number of the pulses averaged in the experiment. In a steady state experiment, N is the ratio of the instrumental response time, such as the RC constant of a lock-in amplifier, and the sample's memory time.

Since $|dR(t_1, t_2)/dt_1| \ll |R/\tau_c|$, we can further replace $g(t_1-\tau)$ by $\tau_c\delta(t_1-\tau)$. Eq. (4.2) then becomes

$$P(\boldsymbol{k}_s, t; \tau) = -i\tau_c E(t-2\tau) \int_0^\infty dt_2\, \langle |E(t-t_2-2\tau)|^2\rangle R(\tau, t_2)$$

$$= -i\mu^4 \rho_c \rho_1 \tau_c E(t-2\tau) \exp(-\gamma\tau) \int_0^\infty dt_2\, \langle |E(t-t_2-2\tau)|^2\rangle\, A(t_2)\, C(\tau, t_2, \tau)\,. \tag{4.10}$$

By comparing eq. (4.10) with eq. (4.7), we see immediately the accumulative nature of the incoherent photon echo. In the absence of TLS-induced dephasing, $C(\tau, t_2, \tau)$ is equal to unity, and the incoherent photon echo will give the same result as a two-photon echo experiment. In glasses, or other systems which have spectral diffusion, however, the results of the incoherent echo can be substantially different from the two-pulse echo because of the integral which contains the four-point correlation function.

To illustrate the differences between accumulated echo experiments, both the conventional ones using mode-locked lasers and those using incoherent light sources, and two-pulse photon echo experiments, consider the following concrete examples.

Case 1: $\beta\Theta = (2\text{ ps})^{-1}$; the accumulated photon echo experiment is performed using a broad band laser with $\tau_c \ll 2$ ps, and a pulse duration $t_d = 10$ ns, $1/t_d > R_{min}, \gamma, \gamma_{ca}$; the detected echo signal is integrated over the laser pulse. In this case, a two-pulse echo measurement yields a homogeneous dephasing rate, $1/T_2 = \beta\Theta/2$. Using the four-point correlation function derived in section 3,

$$C(\tau, t_2, \tau) = \exp[-\beta\tau(\Theta + \ln(1+t_2/\tau)]\,, \tag{4.11}$$

we find that in addition to the exponential decay function measured by the two-pulse photon echo, there is another dephasing term in the accumulated echo polarization,

$$P(\boldsymbol{k}_s, t; \tau) \propto \exp(-\gamma\tau - \beta\Theta\tau)\, D(t; \tau)\,, \tag{4.12}$$

$$D(t; \tau) = \{[1+(t-2\tau)/\tau]^{1-\beta\tau} - 1\}\tau/(1-\beta\tau)\,,$$

where $2\tau<t<t_d+2\tau$. For a fixed τ, eq. (4.12) describes the nature of the incoherent echo if it is observed at a particular time, t, during the laser pulse. We note that different parts of the laser pulse measure different dephasing rates. In our example, however, the observation is the integrated intensity of the incoherent echo signal as a function of the delay time, τ. The normalized decay function is given by

$$S(t_d;\tau)=S_{TPE}(\tau)\,S_1(t_d;\tau)\,, \tag{4.13}$$

$$S_{TPE}(\tau)=\exp[-2(\gamma+\beta\Theta)\tau]\,,$$

$$S_1(t_d;\tau)=\int_{2\tau}^{t_d+2\tau}|D[t;\tau]|^2\,dt\left(\int_{2\tau}^{t_d+2\tau}|D(t;0)|^2\,dt\right)^{-1}. \tag{4.13'}$$

Because of the accumulative effect, the dominant part of the signal is generated by the end portion of the laser pulse. We can write the normalized decay function as

$$S(t_d;\tau)\approx S_{TPE}(\tau)\,|D(t_d;\tau)/D(t_d;0)|^2=\exp[-2(\gamma+\beta\Theta)\tau]\,\exp\{-2[\beta\tau\ln(\tau_d/\tau)-\ln(1-\beta\tau)]\}\,. \tag{4.14}$$

One may notice that eq. (4.14) does not describe an exponential decay. As can be seen in fig. 1, however, a plot of eq. (4.14) appears approximately exponential. Given signal-to-noise ratio considerations in experiments, it is unlikely that a measurement of eq. (4.13) could be distinguished from an exponential decay in an actual experiment. Fig. 1 also displays a plot of the two-pulse photon echo decay for the case 1 example. The major difference in dephasing times measured by the two-pulse photon echo and incoherent echo experiments is clear.

Writing $S_1(t_d;\tau)=\exp(-4\Gamma_1\tau)$, and replacing τ with $1/\beta\Theta$, we calculate that the ratio of the dephasing rate measured by the incoherent photon echo and the dephasing rate measured by the two-pulse photon echo is approximately

$$[\Theta+\ln(t_d\beta\Theta)-1]/\Theta\approx 3\,.$$

This value differs from the numerically calculated value (integration over the pulse was performed, see discussions below) by only a few percent.

Case 2: $\beta\Theta=\gamma=(1\text{ ns})^{-1}$, and the bottleneck state lifetime $1/\gamma_{ca}=50\ \mu s<1/R_{min}$; the accumulated photon echo is performed using a mode-locked laser that produces a constant stream of short pulses (steady state mea-

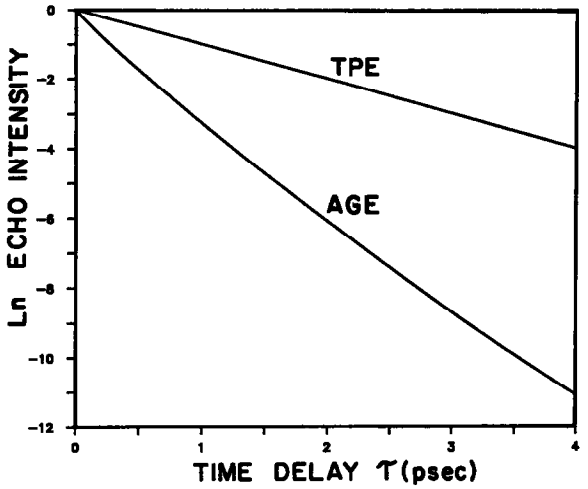

Fig. 1. Normalized signal intensities versus the delay time, τ, as measured by an incoherent echo (lower curve) and by a two-pulse photon echo (upper curve). The incoherent echo signal is plotted using eq. (4.14). Although this curve is not exactly exponential, given signal-to-noise considerations in an experiment, it is unlikely that the non-exponential nature of the decay could be observed. The parameters for both curves are those given in case 1 (see text). This figure illustrates the significant differences which can be observed with an incoherent echo and a two-pulse photon echo in systems which undergo spectral diffusion.

surement). Since in low-temperature glasses the pure dephasing arises almost entirely from TLS-induced fluctuations, we have $\gamma=\gamma_b$. Following the same procedure as in case 1, we find that the additional dephasing term is given by

$$S_1(\infty;\tau)\approx S_1(1/\gamma_{ca};\tau)\approx\exp\{-2[\beta\tau\ln(1/\gamma_{ca}\tau)-\ln(1-\beta\tau)]\}\,.$$

The ratio of the pure dephasing rates measured by the accumulated photon echo and by the two-pulse photon echo is approximately

$$\{\Theta+\ln[(\gamma+\beta\Theta)/\gamma_{ca}]-1\}/\Theta\approx 4\,.$$

We note that the two examples given here use parameters similar to those found in real systems (see, for example, refs. [27,8]).

As can be seen from these examples, both the incoherent and the conventional accumulated photon echoes are sensitive to time scales (typically) much longer than the measured dephasing times. By defining a time variable, t_{max}, to be the shorter of the laser irradiation duration and the sample's memory time, we can state our general results as follows. For $t_{max}<1/R_{min}$, an accumulated photon echo experiment always measures a dephasing rate faster than that measured in a two-pulse photon echo experiment by a factor of $\ln[(\beta\Theta+\gamma)t_{max}]$. For $t_{max}>1/R_{min}$, the factor is given by $\ln[(\beta\Theta+\gamma)/R_{min}]$. The exact details of these predictions are based on the assumption of a constant tunneling parameter distribution in the TLS model. Analogous results will be obtained for other forms of the TLS distribution functions.

The results given above suggest that the distribution of relaxation relates in a complex system such as a glass can be mapped out by performing a series of experiments on different time scales. As an illustration, we consider an accumulated echo experiment in which the laser irradiation time is continuously variable from 1 ns to 1 ms. One can accomplish this by electro-optically or acousto-optically chopping out a pulse from a quasi-continuous broad band laser source to perform incoherent echo experiments on relatively fast time scales. For long laser irradiation times ($t_d>100$ ns), the quasi-continuous broad band laser source can be replaced by a mode-locked laser. The detected echo signal is integrated over the laser irradiation time. We will use the same parameters as in the case 1 and case 2 examples discussed above, except that now the bottleneck state lifetime is taken to be much longer than 1 ms. If the inverse of the minimum relaxation rate of the TLS is longer than the maximum laser irradiation time used in the experiment, $1/R_{min}>(t_d)_{max}$, the measured decay function is given by eq. (4.13), which is a function of both the temporal separation of the two laser beams, τ, and the laser irradiation time duration, t_d. Writing $S_1(t_d;\tau)=\exp(-4\Gamma_1\tau)$, and replacing τ with $(\gamma+\beta\Theta)^{-1}$, we numerically calculated the integrals in eq. (4.13'), and hence the extra dephasing rate, Γ_1. In fig. 2 we plot, as a function t_d, the ratio of the pure dephasing rate measured by the accumulated echo experiment and that measured by a two-pulse echo experiment,

$$\Gamma_{AGE}/\Gamma_{TPE}=(\beta\Theta+2\Gamma_1)/\beta\Theta\,.$$

In both cases, the ratios increase almost linearly with $\ln(t_d)$ for the larger valves of t_d.

Fig. 2 illustrates the nature of measurements over a range of time scales. The plots demonstrate that the dephasing rates measured by the accumulated echo techniques are the same as that measured by the two-pulse photon echo when t_d is comparable to or shorter than the homogeneous dephasing time. However, for such a t_d, the accumulative effect becomes very small, and one can achieve a much better signal-to-noise ratio using the two-pulse photon echo technique. The plots also demonstrate that this type of measurement, combined with a two-pulse photon echo measurement, can be used to obtain information on the distributions of relaxation rates in glasses and in other types of disordered systems, such as complex crystals [16] and proteins [28]. In glasses, the distribution function of relaxation rates is determined by the TLS parameter distribution functions, hence further information about the TLS can also be obtained from these measurements.

Specifically, one can examine the dephasing behavior of the chromophore–glass system around $t_d\approx 1/R_{min}$. In real physical systems, the relaxation rate distribution may slowly approach zero rather than having a sharp

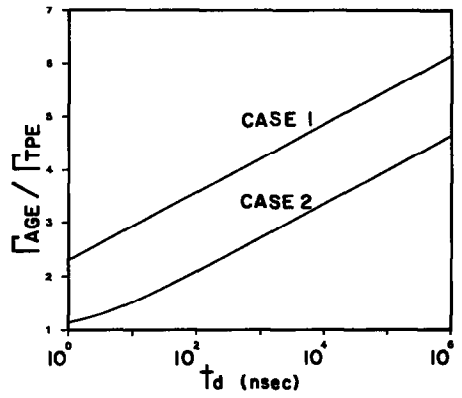

Fig. 2. Calculated ratio of the pure dephasing rate measured by an accumulated echo and that measured by a two pulse-photon echo as a function of the laser irradiation duration, t_d, used in the accumulated echo experiment. The parameters used in the calculations are those given in case 1 and case 2 (see text), except here we have let the bottleneck state lifetime, $1/\gamma_{ca} > (t_d)_{max}$. This figure demonstrates that results from experiments analogous to these calculations can be used to map out the distribution of relaxation rates in a system. The curves also demonstrate that, in a system such as a glass which has spectral diffusion, an accumulated echo experiment only measures the same dephasing time as a two-pulse photon echo in the limit that the laser irradiation time used in the accumulated echo experiment is short relative to the homogeneous dephasing time (which is measured by the two-pulse photon echo).

cut off at R_{min}. If the falling slope is slower than the falling edge of the function $f(R\tau, Rt_2)$, one should be able to map out the relaxation rate distribution in the region about R_{max}, and the tunneling parameter distribution in the region about λ_{max}. This is due to the fact that as t_d is increased, the ratio of the dephasing rate will eventually reach a saturation point at $t_d \approx 1/R_{min}$. This can be seen from the definition of our four-point correlation function in eq. (3.15). The integral variable t in eq. (4.13′) should be replaced by $t' = \min(t, 1/R_{min})$. The behavior of eq. (4.13) around $t_d \approx 1/R_{min}$ should reveal the behavior of the falling edge of the tunneling parameter distribution function. On very long time scales, it may be preferable to make this type of long time scale measurement using time-dependent optical hole burning experiments rather than accumulated photon echo techniques. The relationship between the time scale of a hole burning experiment and the observed dephasing time is analogous to that described here for accumulated echo experiments [8]. In a similar manner, one could reveal the behavior of the relaxation rate distribution function around R_{max} by measuring the two-pulse echo dephasing on a very short time scale, $\tau < 1/R_{max}$, with ultrashort laser pulses. In this case, one should see the echo signal decay rate changes from slow to fast as the pulse separation τ increases and passes the point of $1/R_{max}$.

We would like to point out that the relation between the exponential decay of the two pulse echo in glasses and $1/R$ fluctuation rate distributions was first recognized by Maynard et al. [29]. Their derivation used the sudden jump model developed in ref. [15], hence gives a more accurate two-pulse echo decay rate. The corresponding two-pulse echo decay constant Θ is found to be 2.6, instead of 3.6 used in ref. [8] and in this work. If the value 2.6 is used, the ratios of the decay rates evaluated above in the two examples should be 4 and 5, instead of 3 and 4 as in the text.

Acknowledgement

The authors would like to thank Professor Mark Berg for the helpful comments on the paper. This work was supported by the office of Naval Research (#N00014-86-K-0825) and by the National Science Foundation, Division of Materials Research (#DMR87-18959).

Appendix A

Following ref. [25], we write the nonlinear response function as a matrix element in the Liouville space,

$$R(t_3, t_2, t_1) = \mu_{ab} \ll ba | G(t_3+t_2+t_1, t_2+t_1) U G(t_2+t_1, t_1) U G(t_1, 0) U | aa \gg . \quad (A.1)$$

For simplicity, we have omitted the index i. The double bracket in the equation denotes an average in the Liouville space. $|\alpha\beta\rangle\!\rangle$ is short hand for $\|\alpha\rangle\langle\beta|\rangle\!\rangle$. The perturbation operator U is defined as $UA=-[\mu, A]$, where A is an arbitrary linear operator. The evolution operator of the unperturbed system between times t_1 and t_2 is $G(t_1, t_2)=\exp[-iL(t_2, t_1)]$, where the Liouville operator L is defined as $LA=[H_0, A]$. And we have assumed that the chromophore is initially in the ground state, $\rho(-\infty)=|a\rangle\langle a|$.

The derivation of R is essentially the same as calculating the time evolution of the density matrix, ρ. The two methods are readily related by $\rho_{\alpha\beta}=\langle\langle\alpha\beta|\rho\rangle\rangle$. In our case, the coherence propagation is along a path,

$$aa \xrightarrow{U} ab \xrightarrow{G} \xrightarrow{U} aa, bb \xrightarrow{G} \xrightarrow{U} ba \xrightarrow{G},$$

where the letter above each arrow indicates the operator responsible for the propagation. Thus we can write

$$R(t_3, t_2, t_1)=\mu_{ab}\langle\langle ba|G(t_3+t_2+t_1, t_2+t_1)|ba\rangle\rangle\langle\langle ba|$$
$$\times U\sum_{\alpha=a.b}|\alpha\alpha\rangle\rangle\langle\langle\alpha\alpha|G(t_2+t_1, t_1)\sum_{\alpha=a.b}|\alpha\alpha\rangle\rangle\langle\langle\alpha\alpha|U|ab\rangle\rangle\langle\langle ab|G(t_1, 0)|ab\rangle\rangle\langle\langle ab|U|aa\rangle\rangle . \tag{A.2}$$

The relevant matrix elements of $U(-[\mu,])$ are given by

$$\langle\langle ab|U|aa\rangle\rangle=\mu_{ab}, \quad \langle\langle aa|U|ab\rangle\rangle=\langle\langle ba|U|aa\rangle\rangle=\mu_{ba}, \quad \langle\langle bb|U|ab\rangle\rangle=\langle\langle ba|U|bb\rangle\rangle=-\mu_{ba}. \tag{A.3}$$

The off-diagonal term of G is given by

$$\langle\langle ab|G(t_2, t_1)|ab\rangle\rangle=\exp\left(i\omega_{ab}(t_2-t_1)+i\int_{t_1}^{t_2}\Delta\omega(t')\,dt'-\gamma(t_2-t_1)/2\right), \tag{A.4}$$

where $\Delta\omega(t')=\Delta(s)+\Delta(t')$, and $\gamma/2=\gamma_b/2+\Gamma'$, Γ' accounts for dephasing from processes other than coupling to the TLS. The diagonal terms are found by solving the rate equations for the populations. Taking $\gamma_{ba}\gg\gamma_{ca}$ gives

$$\langle\langle aa|G(t_2, t_1)|aa\rangle\rangle=1,$$
$$\langle\langle bb|G(t_2, t_1)|bb\rangle\rangle=\exp[-\gamma_b(t_2-t_1)],$$
$$\langle\langle aa|G(t_2, t_1)|bb\rangle\rangle=\phi_a\{1-\exp[-\gamma_b(t_2-t_1)]\}+\phi_c\{1-\exp[-\gamma_{ca}(t_2-t_1)]\},$$
$$\langle\langle bb|G(t_2, t_1)|aa\rangle\rangle=0, \tag{A.5}$$

where $\phi_a=\gamma_{ba}/\gamma_b$, and $\phi_c=\gamma_{bc}/\gamma_b$.

Substituting eqs. (A.3)–(A.5) to eq. (A.2), denoting $|\mu_{ab}|$ by μ, and retrieving the index i, we find

$$R_i(t_3, t_2, t_1)=\mu_i^4\exp\{i[\omega_{ab}+\Delta_i(s)](t_1-t_3)-\gamma(t_1+t_3)/2\}A(t_2)\,C_i(t_3, t_2, t_1),$$
$$A(t_2)=2\exp(-\gamma_b t_2)+\phi_c[\exp(-\gamma_{ca}t_2)-\exp(-\gamma_b t_2)],$$
$$C_i(t_3, t_2, t_1)=\exp\left(-i\int_{t_2+t_1}^{t_3+t_2+t_1}\Delta_i(t')\,dt'+i\int_0^{t_1}\Delta_i(t')\,dt'\right). \tag{A.6}$$

Appendix B

The variance of the phase perturbation from the TLS can be explicitly written in terms of frequency perturbation

$$\sigma^2(\varphi)=\left(\int_{t_2+t_1}^{t_2+2t_1}\delta\Delta(t')\,dt'-\int_0^{t_1}\delta\Delta(t')\,dt'\right)^2$$

$$=2\left(2\int_0^{t_1}(t_1-t')g(t')\,dt'-\int_{t_2}^{t_2+t_1}(t'-t_2)g(t')\,dt'-\int_{t_2+t_1}^{t_2+2t_1}(t_2+2t_1-t')g(t')\,dt'\right). \tag{B.1}$$

Here we have assumed that the fluctuations of the TLS are not affected be the chromophore's behavior, hence they can be taken as a stationary stochastic process. This implies that the covariance of the perturbation, $g(t, t')=\langle\delta\Delta(t)\,\delta\Delta(t')\rangle$, is in the form $g(t, t')=g(t'-t)=g(t-t')$. $\delta\Delta(t)$ is defined as $\Delta(t)-\langle\Delta(t)\rangle$, and is proportional to the population fluctuation of the TLS relative to its equilibrium.

We reason that the covariance, $\langle\delta\Delta(t)\,\delta\Delta(t')\rangle$, should obey a Markoffian process,

$$\langle\delta\Delta(t;E,\lambda)\,\delta\Delta(t';E,\lambda)\rangle=\langle[\delta\Delta(t;E,\lambda)]^2\rangle\exp(-R(E,\lambda)|t-t'|)\,, \tag{B.2}$$

$$\langle[\delta\Delta(t;E,\lambda)]^2\rangle\equiv\sigma^2(\Delta)\,.$$

The argument is as follows. We recall the phenomenological interaction Hamiltonian in eq. (2.1′). $\Delta(t)$ is directly related to the population difference of the TLS by $\Delta(t;E,\lambda)\propto\Delta\rho(t;E,\lambda)$. Solving the equation of motion of the TLS, we have

$$\Delta\rho(t';E,\lambda)-\Delta\rho(\mathrm{eq};E,\lambda)=[\Delta\rho(t;E,\lambda)-\Delta\rho(\mathrm{eq};E,\lambda)]\exp[-R(E,\lambda)(t'-t)]\,, \tag{B.3}$$

where $t'>t$. Eq. (B.2) is a direct result of this relation.

Since the actual tunneling process of the TLS takes place in a much shorter time than the relaxation time $1/R$, it can be modeled as a sudden "jump" between its levels. Thus $\Delta(t)$ takes discrete values: $+\Delta_0$ for excited state and $-\Delta_0$ for the ground state. Following eq. (2.1′), Δ_0 is defined as the amplitude of the coupling strength between the TLS and the chromophore, $\Delta_0=\xi_b-\xi_a=\Delta_0(E,\lambda,r)$. This bistable nature suggests that $\Delta(t)$ has a mean value $\langle\Delta(t)\rangle=\Delta_0[2\rho_{11}(\mathrm{eq})-1]$ and a variance

$$\sigma^2(\Delta)=4\rho_{11}(\mathrm{eq})[1-\rho_{11}(\mathrm{eq})]\Delta_0^2\,, \tag{B.4}$$

where $\rho_{11}(\mathrm{eq})$ is the probability at equilibrium of finding the TLS in its excited state

$$\rho_{11}(\mathrm{eq})=\exp(-E/kT)/[1+\exp(-E/kT)]\,.$$

Thus the variance of $\Delta(t)$ can be explicitly written as

$$\sigma^2(\Delta)=\mathrm{sech}^2(E/2kT)\Delta_0^2\,. \tag{B.5}$$

Substituting eqs. (B.2) and (B.5) to eq. (B.1), after some manipulation, we have

$$\sigma^2(\varphi)=2[\sigma(\Delta)t_1 f(Rt_1,Rt_2)]^2\,, \tag{B.6}$$

$$f(Rt_1,Rt_2)=(\sqrt{2}/Rt_1)\{\exp(-Rt_1)-(1-Rt_1)-\exp[-R(t_2+t_1)][\cosh(Rt_1)-1]\}^{1/2}\,.$$

Appendix C

In the $\ln(R)$ scale, the relaxation distribution function is a constant in the region $(R_{\min}, R_{\max})$. One can evaluate the average of the function

$$f(Rt_1,Rt_2)=(\sqrt{2}/Rt_1)\{\exp(-Rt_1)-(1-Rt_1)-\exp[-R(t_2+t_1)][\cosh(Rt_1)-1]\}^{1/2} \tag{C.1}$$

by examining its behavior in the $\ln(R)$ scale. In fig. 3, we plot the functions $f(Rt_1, 0)$, $f(Rt_1, Rt_2)$, and $f(Rt_1,$

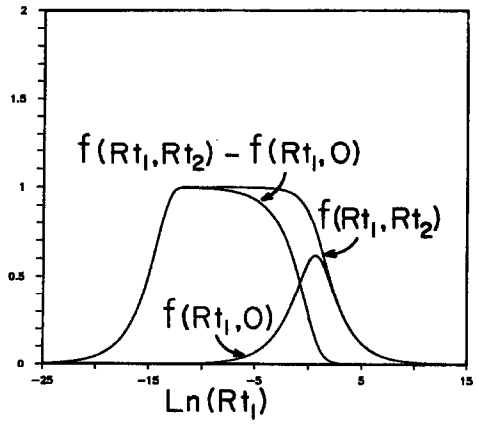

Fig. 3. Functions f plotted against a $\ln(Rt_1)$ scale. The ratio of the two characteristic time scales is set to be $t_2/t_1 = 10^6$.

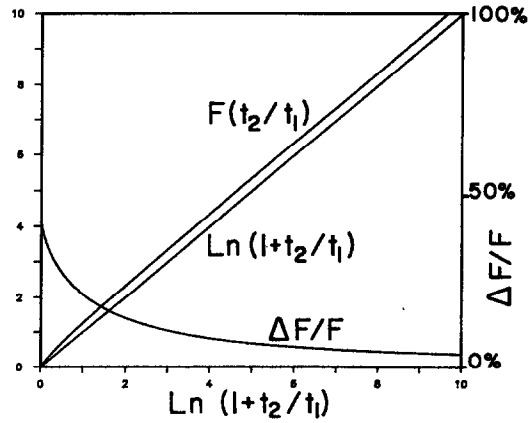

Fig. 4. Parametric integral $F(t_2/t_1)$ and the relative error $\Delta F/F$ versus $\ln(1+t_2/t_1)$.

$Rt_2)-f(Rt_1, 0)$ in the scale of $\ln(Rt_1)$. If the ratio t_2/t_1 is large, $f(Rt_1, Rt_2)-f(Rt_1, 0)$ can be approximated by a step function

$$f(Rt_1, Rt_2)-f(Rt_1, 0)\approx H(R-B_1/t_1)H(B_2/t_2-R)\,, \tag{C.2}$$

where B_1 and B_2 are constants on the order of unity. As t_2/t_1 increases, the contributions of the edges to the integral become negligible. Thus this is quite a good approximation for large t_2/t_1. Note that this equation is equivalent to eq. (50) in ref. [8]; however, due to an algebraic error, the latter is off by a factor of $\sqrt{2}$.

To extend this approximation to small t_2/t_1, we write

$$f(Rt_1, Rt_2)-f(Rt_1, 0)\approx H(R-B_1/t_1)H[B_2'/(t_1+t_2)-R]\,. \tag{C.3}$$

Since we are mainly interested in the integral of this function over $\ln(R)$, we will only evaluate the error in the integral introduced by this approximation. The integral of the right side of eq. (C.3) over $\ln(R)$ is given by $\ln(1+t_2/t_1)+\ln(B_1/B_2')$. The left side of eq. (C.3) gives a parametric integral

$$F(t_2/t_1)=\int_0^\infty \mathrm{d}R\{f(Rt_1, Rt_2)-f(Rt_1, 0)\}/R\,, \tag{C.4}$$

which can be performed numerically. Both integrals should be equal to zero for $t_2=0$. Thus we conclude that $B_2'=B_1$. In fig. 4, we plot the parametric integral $F(t_2/t_1)$ versus $\ln(1+t_2/t_1)$. The relative error introduced by this approximation, $[F(t_2/t_1)-\ln(1+t_2/t_1)]/F(t_2/t_1)$, is also plotted. As can be seen, the error is never larger than 8% for $t_2/t_1 > 10$.

References

[1] M.J. Weber, J. Luminescence 36 (1987) 179.
[2] W.A. Phillips, ed., Amorphous solids: low-temperature properties (Springer, Berlin, 1981).
[3] P.W. Anderson, B.I. Halperin and C.M. Varma, Phil. Mag. 25 (1972) 1.
[4] W.A. Phillips, J. Low Temp. Phys. 7 (1972) 351.
[5] R.O. Pohl, Amorphous solids: low-temperature properties, ed. W.A. Phillips (Springer, Berlin, 1981) p. 27; M.O. Birge and S.R. Nagel, Phys. Rev. Letters 54 (1985) 2674.

[6] N.A. Kurnit, I.D. Abella and S.R. Hartmann, Phys. Rev. Letters 13 (1964) 567.
[7] W.H. Hesselink and D.A. Wiersma, Phys. Rev. Letters 43 (1979) 1991; J. Chem. Phys. 75 (1981) 4192.
[8] M. Berg, C.A. Walsh, L.R. Narasimhan, K.A. Littau and M.D. Fayer, J. Chem. Phys. 88 (1988) 1564.
[9] S. Asaka, H. Nakatsuka, M. Fujiwara and M. Matsoka, Phys. Rev. A 29 (1984) 2286.
[10] N. Morita and T. Yajima, Phys. Rev. A 30 (1984) 2525.
[11] R. Beach and S.R. Hartmann, Phys. Rev. Letters 53 (1984) 663.
[12] N. Morita, T. Tokizaki and T. Yajima, J. Opt. Soc. Am. B 4 (1987) 1269, and references therein.
[13] J.R. Klauder and P.W. Anderson, Phys. Rev. 125 (1962) 912.
[14] W.B. Mims, Phys. Rev. 168 (1968) 378.
[15] P. Hu and S.R. Hartmann, Phys. Rev. B 9 (1974) 1;
P. Hu and L.R. Walker, Phys. Rev. B 18 (1978) 1300.
[16] R.M. Macfarlane and R.M. Shelby, in: Laser spectroscopy, Vol. 6, eds. H.P. Weber and W. Lüthy (Springer, Berlin, 1983) p. 113.
[17] B. Golding and J.E. Graebner, in: Amorphous solids; low-temperature properties, ed. W.A. Phillips (Springer, Berlin, 1981).
[18] J.L. Black and B.I. Halperin, Phys. Rev. B 16 (1977) 2879.
[19] S. Hunklinger and M. Schmidt, Z. Physik B 54 (1984) 93.
[20] D.L. Huber, M.M. Broer and B. Golding, Phys. Rev. Letters 52 (1984) 2281.
[21] W.O. Putikka and D.L. Huber, Phys. Rev. B 36 (1987) 3436.
[22] K.K. Rebane and A.A. Gorokhovskii, J. Luminescence 36 (1987) 237.
[23] D.E. McCumber and M.D. Sturge, J. Appl. Phys. 81 (1984) 1604.
[24] D. Hsu and J.L. Skinner, J. Chem. Phys. 81 (1984) 1604.
[25] S. Mukamel and R.F. Loring, J. Opt. Soc. Am. B 3 (1986) 595;
S. Mukamel, Phys. Rev. A 28 (1983) 3480.
[26] P.W. Anderson and P.R. Weiss, Rev. Mod. Phys. 25 (1953) 269.
[27] C.A. Walsh, M. Berg, L.R. Narasimhan, K.A. Littau and M.D. Fayer, Chem. Phys. Letters 134 (1987) 268.
[28] J.O. Alben et al., Proc. Natl. Acad. Sci. US 79 (1982) 3744.
[29] R. Maynard, R. Rammal and R. Suchail, J. Phys. Letters 41 (1980) L-291.